Geomechanics and Engineering, *Vol. 37, No. 1 (2024) 31-48*
https://doi.org/10.12989/gae.2024.37.1.031

A simplified framework for estimation of deformation pattern in deep excavations

Abdollah Tabaroei*[1] and Reza Jamshidi Chenari[2a]

[1]*Department of Civil Engineering, Eshragh Institute of Higher Education, Bojnourd, Iran*
[2]*Senior Geotechnical Engineer, TREK Geotechnical Inc., Manitoba, Canada*

(*Received March 14, 2023, Revised December 28, 2023, Accepted March 8, 2024*)

Abstract. To stabilize the excavations in urban area, soil anchorage is among the very common methods in geotechnical engineering. A more efficient deformation analysis can potentially lead to cost-effective and safer designs. To this end, a total of 116 three-dimensional (3D) finite element (FE) models of a deep excavation supported by tie-back wall system were analyzed in this study. An initial validation was conducted through examination of the results against the Texas A&M excavation cases. After the validation step, an extensive parametric study was carried out to cover significant design parameters of tie-back wall system in deep excavations. The numerical results indicated that the maximum horizontal displacement values of the wall (δ_{hm}) and maximum surface settlement (δ_{vm}) increase by an increase in the value of ground anchors inclination relative to the horizon. Additionally, a change in the wall embedment depth was found to be contributing more to δ_{vm} than to δ_{hm}. Based on the 3D FE analysis results, two simple equations are proposed to estimate excavation deformations for different scenarios in which the geometric configuration parameters are taken into account. The model proposed in this study can help the engineers to have a better understanding of the behavior of such systems.

Keywords: excavation; horizontal displacement of the wall; surface settlement; tie-back wall; wall embedment depth

1. Introduction

Due to the rapid urban growth and paucity of construction sites in urban areas, demand for high-rise buildings is soaring. The construction of such buildings is also associated with excavating deep into the ground. Although numerous studies have been dedicated to investigate the behavior of retaining structures utilized under such circumstances, local or global failures in the excavation process still leave financial losses and mortalities behind. This matter highlights further revisitiry the design and construction process for temporary retaining systems. Selection of the structural element generally depends on the subsurface soil type, ground water conditions, local construction practice, and availability of material and equipment, and performance requirements. One of the common choices is the tie-back wall, which is influenced by parameters such as the excavation technique, the installation method and material type of the ground anchors.

Earlier studies have discussed the use of finite and discrete elements in geotechnical engineering (Tabaroei and Ghazavi 2013, Sarfarazi and Tabaroei 2020, Sarfarazi *et al.* 2022, Tabaroei *et al.* 2022, Tabaroei *et al.* 2023). To control and limit the wall deflections and ground surface settlements triggered by deep excavations, a number of experimental, analytical and FE analyzes have been reported in literature (Ou *et al.* 1996, Ou and Shiau 1998, Ou *et al.* 2000, Zdrakovic *et al.* 2005, Yoo and Lee 2008, Hou *et al.* 2009, Kung 2009, Chowdhury *et al.* 2012, Comodromos *et al.* 2013, Borges and Guerra 2014, Ignat *et al.* 2015, Chowdhury *et al.* 2016, Ding *et al.* 2017, Kim *et al.* 2018, Lee 2019, Liu *et al.* 2020, Ning *et al.* 2021, Karira *et al.* 2022, Wang *et al.* 2023). Blackburn (2005) showed that 3D FE model could predict the deformations of an excavation fairly accurately by comparing the results of numerical models against measurements. Furthermore, some researchers also followed the 3D numerical modeling approach and found that movements caused by excavation reduce near the corners of an excavation (Bono *et al.* 1992; Chew *et al.* 1997, Finno and Bryson 2002, Finno and Roboski 2005). According to the optical survey data obtained around a 12.8 m deep excavation in Chicago, Finno and Roboski (2005) and Roboski and Finno (2006) proposed parallel distributions of settlement and lateral ground movement for deep excavations in soft to medium clays. Using the complementary error function, they also found that geometry and maximum movement parameters are necessary for defining the parallel distributions of ground movement.

Most of studies on tie-back walls (or soil arching system) are based on analytical and numerical modeling (Clough and Tsui 1974, Simpson *et al.* 1979, Mosher and Knowles 1990, Chung and Briaud 1993, Briaud and Lim 1999, Dawkins *et al.* 2003, Abraham 2007, Orazalin 2012, Muntohar and Liao 2013, Ahmadi and Ahmadi 2019, Tabaroei *et al.* 2022). Mosher and Knowles (1990) studied a

*Corresponding author, Assistant Professor
E-mail: a.tabaroei@eshragh.ac.ir
[a]Associate Professor
E-mail: Jamshidi_reza@guilan.ac.ir

ISSN: 2005-307X (Print), 2092-6219 (Online)

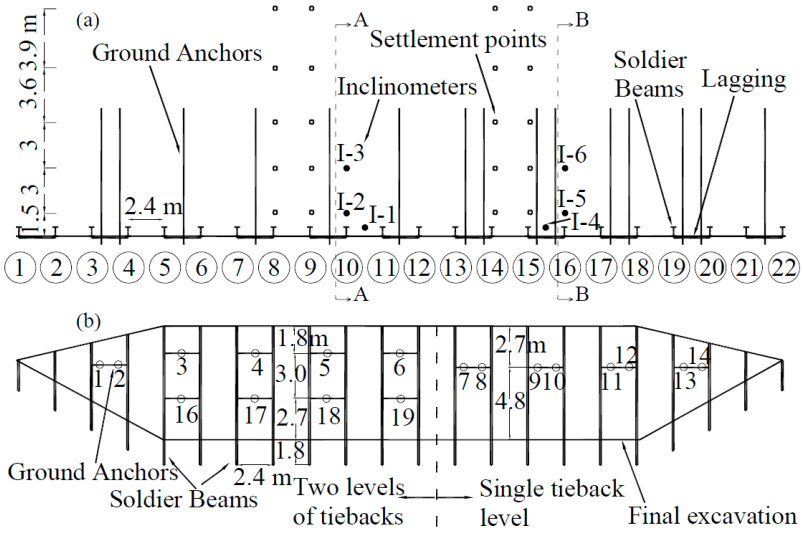

Fig. 1 Schematic of the Texas A&M University full scale model excavation site (Weatherby *et al.* 1998); (a) plan view and instruments layout and (b) elevation view of the wall

15.24 m high temporary tie-back reinforced concrete diaphragm wall by FE analysis and showed that the relative value of the hyperbolic soil stiffness modulus is a significant parameter influencing the results of numerical models. Briaud and Lim (1990) reported that the position of the first anchors had very little effect on the axial loads. Additionally, they indicated that the location of the tendon bonded length only had a small effect on the bending moment and axial load in the soldier piles as long as this length is outside the failure wedge. Orazalin (2012) showed that 3D FE analysis can be effectively used to investigate the complex excavation projects and is capable of achieving consistent predictions on wall deflections, ground movements, pore pressures for tie-back, corner-braced, and raker supported of diaphragm walls. Muntohar and Lio (2013) carried out some 2D FE analyses to demonstrate satisfactory modelling tied-back diaphragm wall using elasto-plastic Mohr-Coulomb soil model. Their results also corroborated that the maximum horizontal displacement occurred at around the bottom of diaphragm wall. Ahmadi and Ahmadi (2019), by using PLAXIS 2D and FLAC 3D, showed that 2D modeling lacks the ability to simulate the positive effect of arching; hence, contending 2D simulation to overestimate the wall deflection and rendering economically less viable designs. Tabaroei *et al.* (2022) by conducting some 3D FE analysis showed that the value of horizontal displacement at upper part of the wall is highly sensitive to the position of the first row of anchor.

While numerous studies have explored the behavior of tie-back walls, there remains a lack of systematic research on the critical parameters influencing their design. This study delves into the behavior of tie-back walls using extensive 3D numerical models. A total of 116 distinct 3D models were created to analyze the influence of various design parameters. The deformations derived from these models were subsequently used to formulate a concise mathematical relationship for tie-back wall displacement parameters.

2. Case study and numerical model

Given that the numerical models conducted in the parametric study focus on tie-back walls, the selection of a case study aimed to align with this emphasis. After careful evaluation of previous studies, the Texas A&M case study was chosen, and a comprehensive 3D modeling analysis was undertaken. To validate the results derived from the 3D model, a comparison was made against measurements and findings from the available study conducted by Briaud and Lim (1999). Within this section, characteristics of the Texas A&M excavation are presented briefly, and the details of 3D numerical modeling are explained accordingly. Finally, the results obtained from 3D numerical modeling using PLAXIS 3D have been compared with the measurements and the results of Briaud and Lim (1999).

2.1 Texas A&M excavation

The Texas A&M full scale model wall with 60 m in length and 7.5 m in height was constructed and tested as a four-episode research with the aim to improve design of permanent ground anchor walls for highway applications (Weatherby *et al.* 1998, Abraham 2007). A test wall contained sections supported by one and two rows of ground anchors (Weatherby *et al.* 1998, Briaud and Lim 1999, Abraham 2007). The wall was built in a line on 2.4 m center by center driven H piles for one part, and the same geometrical feature was maintained for another part of the wall while using drilling and grouting methods of construction (Weatherby *et al.* 1998, Briaud and Lim 1999, Abraham 2007). A plan view of the instrumentation scheme and elevation view of the wall at this site are illustrated in Fig. 1. The cross section of two-level tie-back wall is also shown in Fig. 2. As seen in Fig. 1, up to soldier beam number 12, the piles have lighter sections and therefore two levels of tie-backs were used. For soldier beam numbers 13 to 22 a single tie-back level was used because of the larger

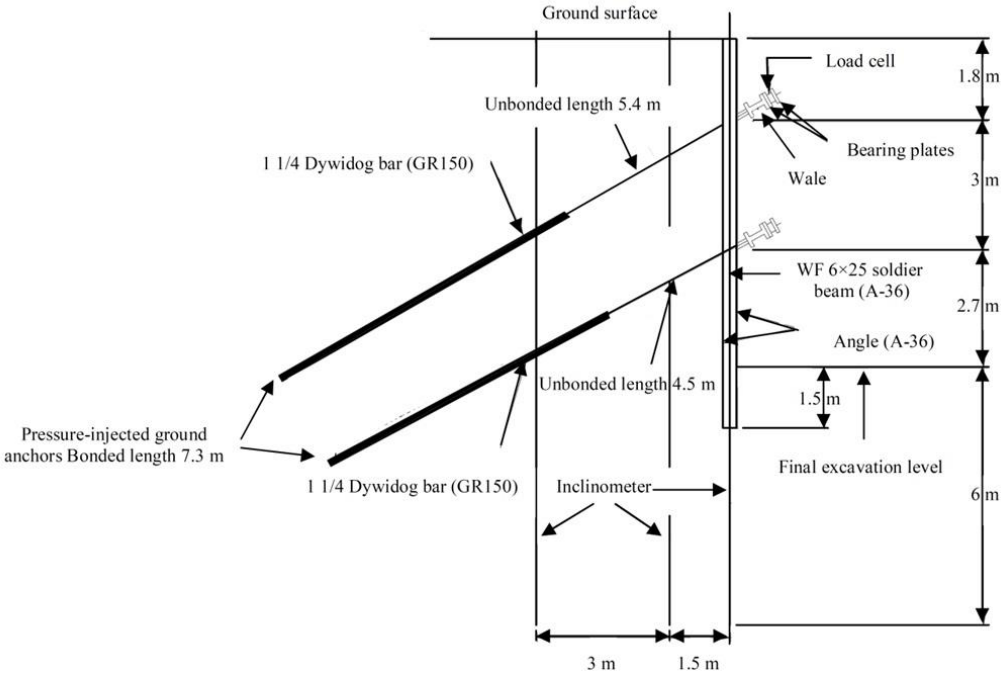

Fig. 2 Section of two levels of tie-back wall of the Texas A&M University excavation (Abraham 2007)

Table 1 Soil parameters used in 3D FEA (Abraham 2007)

Layer No.	Type of soil	γ (kN/m^3)	c (kPa)	φ (°)	E_{50}^{ref} (MPa)	E_{oed}^{ref} (MPa)	E_{ur}^{ref} (MPa)	m (-)	ν (-)	R_f (-)	R_{int} (-)
1	Silty sand	18	0	32	35	35	105	0.8	0.2	0.7	0.9
2	Medium dense sand	18	0	32	15	15	45	0.8	0.2	0.7	0.9
3	Clayey sand	19.6	0.5	32	15	15	45	0.8	0.2	0.7	0.9
4	Hard clay	20.5	500	30	49.25	49.25	147.75	0.8	0.2	0.7	0.9

pile sections. The ground anchors were of high-pressure type and inclined 30° relative to the horizontal direction located at 1.8 and 4.8 m below the top of the wall (Briaud and Lim 1999). The wood lagging was used to support the soil between soldier beams. The length, height and thickness of the wood lagging boards were 2.4 m, 30 cm and 75 mm, respectively. Soldier beams 7 to 10 are reinforced by two levels of tie-backs and soldier beams 13 to 16, reinforced by single level tie-back section, were instrumented with inclinometers and surface settlement pins (Weatherby *et al.* 1998, Abraham 2007). More details on this case are provided in the literature (Weatherby *et al.* 1998, Briaud and Lim 1999, Abraham 2007). In order to perform 3D numerical modeling in this research, the two-level tie-back wall of the Texas A&M excavation is opted.

2.2 Development of 3D numerical model

All numerical modelings in this study were carried out by PLAXIS 3D, which is based on finite element method (FEM); it offers many advantages, such as considering soil-structure interaction (SSI) effects, ability to compute under large deformations formulations, ability of coupled analysis, including different constitutive models, and ability to determine the factor of safety (FS) (PLAXIS 2020). PLAXIS 3D therefor-enabled modeling of the soil, the unbonded and bonded lengths of ground anchors, soldier beams, wood lagging, wall and especially the SSI interaction. The hardening soil (HS) model, a constitutive model in PLAXIS, effectively predicts wall displacement and ground surface settlement in excavation scenarios. Hence, this model is employed in this study. Moreover, the HS model has been utilized in prior research on excavation issues (Huang *et al*. 2013, Chhenga and Likitlersuang 2017, Tabaroei *et al*. 2022). The soil layers and soil parameters used in the numerical modeling of this research are summarized in Table 1. These parameters were taken from Abraham (2007) study.

To simulate soldier beam and wood lagging in 3D FE analyses, the plate element was used. Plates with linear-elastic behavior were composed of six-node triangular plate elements with three translational degrees of freedom (u_x, u_y and u_z) and three rotational degrees of freedom (φ_x, φ_y and φ_z) per node (PLAXIS 2020). Wales were simulated by beam element, and interface element was used to consider the interaction between soldier beam and wood lagging with

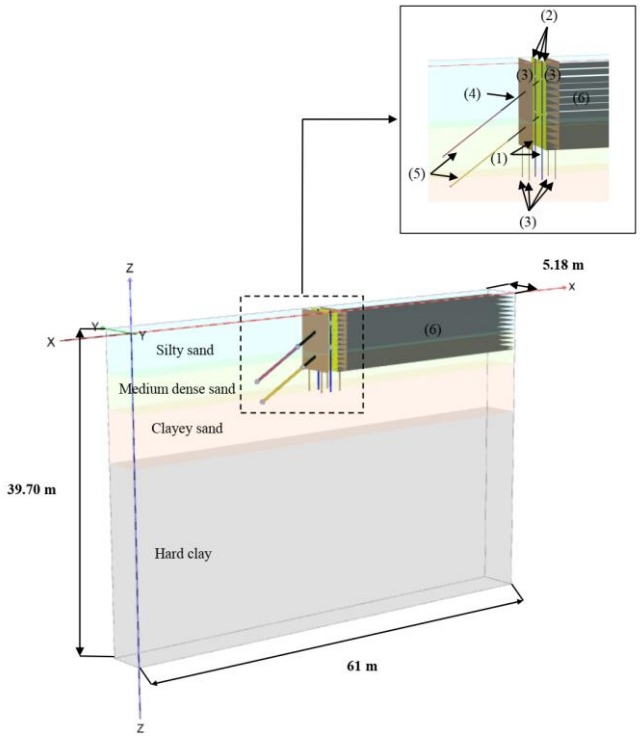

(1) Soldier beam (2) Wood lagging (3) Interface elements (4) Unbonded length of anchor (5) Bonded length of anchor (6) Excavation layers

Fig. 3 3D FE model of the two-level tie-back wall at the Texas A&M excavation and elements used in numerical modeling

Table 2 FE calculations steps in PLAXIS 3D for the two-level tie-back wall at the Texas A&M excavation

Phase No.	Description
0	Generate the initial stress
1	Activate soldier beams and interface elements
2	Excavate to a depth of 0.6 m and place wood lagging
3	Excavate to a depth of 1.2 m and place wood lagging
4	Excavate to a depth of 1.85 m and place wood lagging
5	Place upper wale system
6	Pre-stress the first row of ground anchors
7	Excavate to a depth of 2.4 m and place wood lagging
8	Excavate to a depth of 3 m and place wood lagging
9	Excavate to a depth of 3.6 m and place wood lagging
10	Excavate to a depth of 4.2 m and place wood lagging
11	Excavate to a depth of 4.85 m and place wood lagging
12	Place lower wale system
13	Pre-stress the second row of ground anchors
14	Excavate to a depth of 5.4 m and place wood lagging
15	Excavate to a depth of 6 m and place wood lagging
16	Excavate to a depth of 6.6 m and place wood lagging
17	Excavate to a depth of 7.2 m and place wood lagging
18	Excavate to a depth of 7.5 m and place wood lagging

surrounding soil elements. In 3D FE analysis, ground anchors were simulated by means of a node-to-node anchor and embedded beam elements, where these elements represent the unbonded and bonded length of anchors, respectively. An embedded beam element consists of beam elements with special interface elements providing the interaction between the beam and surrounding soil (PLAXIS 2020). The beam elements are three-node line elements with three translational degrees of freedom and three rotational degrees of freedom per node (PLAXIS 2020). The dimensions of the 3D numerical model were considered according to Abraham (2007). Based on the construction activities of the two-level tie-back wall at the Texas A&M excavation, steps of FE calculations in PLAXIS 3D are presented in Table 2. In Figure 3, 3D FE model of the two-level tie-back wall of Texas A&M excavation is illustrated. The 3D model consists of 24473 ten-node triangular elements with 39468 nodes.

3. Validation of the developed numerical model

Results obtained from the developed numerical model have been validated against the measurements and the results of Briaud and Lim (1999). A comparison between the results of the wall deflection at final stage of excavation are presented in Fig. 4. It is evident that the results of Briaud and Lim (1999) and the current study both are greater than the measurements at almost the entire profile. Reaching correspondence between results obtained from

(2)

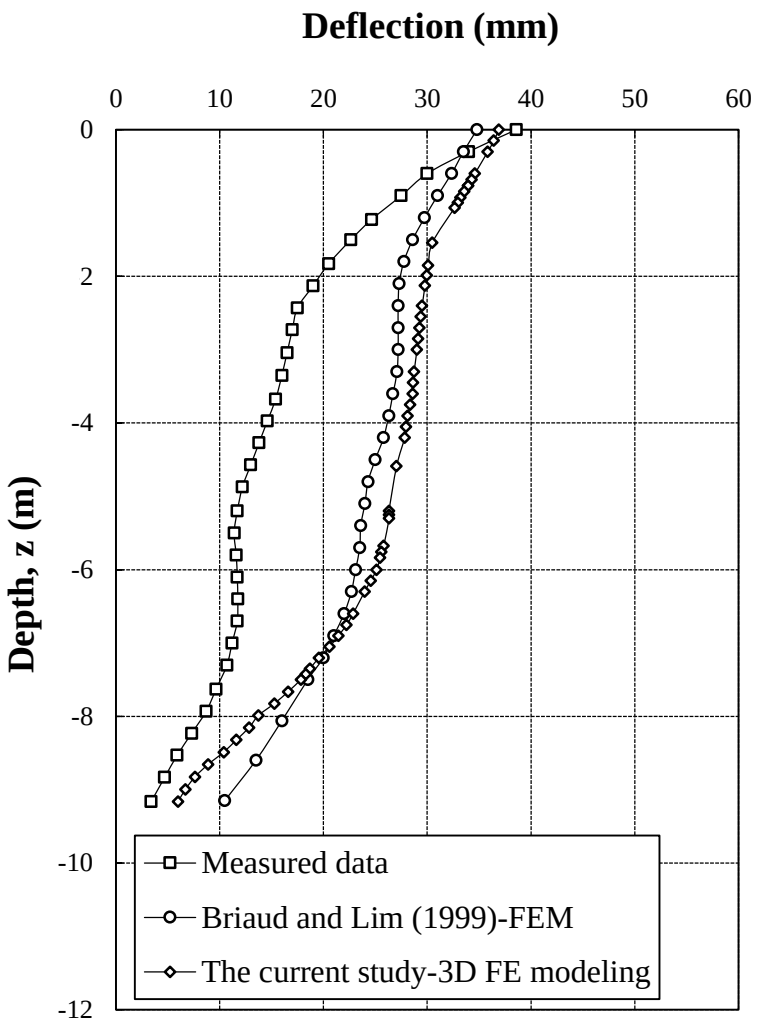

Fig. 4 Comparison between the results obtained from the current study, measurements, and the results of Briaud and Lim (1999)

numerical simulations and in-situ instrumentation measurements poses a considerable challenge, particularly in excavation problems encountered in research endeavors. One important contributing factor to the deviations between the results is the uncertainty associated with determining certain soil parameters and their depth-varying heterogeneity. As detailed in Table 1, the soil parameters utilized in the analysis were derived from the study conducted by Abraham (2007). Other nuances include the construction stages, measurement errors, site investigation issues, facing element modeling, etc. It also illustrates that the wall deflection is larger at shallower depths, bearing witness to a cantilever type behavior. This trend of behavior is not unexpected due to the deep excavation. Fig. 4 shows that the value of deflection occurred at the wall crest is 38.60, 36.88 and 34.80 mm from the measured data, the current study and Briaud and Lim (1999), respectively. Evidently, the results of the current study are largely consistent with those reported by Briaud and Lim (1999) regarding an average deviation of 5.9%. Although the measured data are slightly over predicted by the two numerical methods, the deflections at the extremes (the top and bottom) are well predicted. This reasonable correspondence with literature corroborates the merits of this numerical recipe for further 3D FE analyzes. It should be mentioned that the maximum wall deflection obtained from numerical modeling of this study are lower than the values recommended in FHWA-SA-99-015.

4. Parametric studies and discussion

To examine the response of tie-back walls in deep excavations, a total of 115 3D FE analyzes were conducted, covering different configurations of design parameters. The parameters included the anchors inclination relative to the horizon (θ), the geometric arrangement of ground anchors and embedment depth of the wall. In engineering practice, horizontal displacements of the wall as well as the surface settlements are usually evaluated to control the behavior of the wall during excavation and ensure a safe operation. Details of the parameters using in the 3D FE modelings are presented in Table 3. In addition, the different configurations of ground anchors used in the current

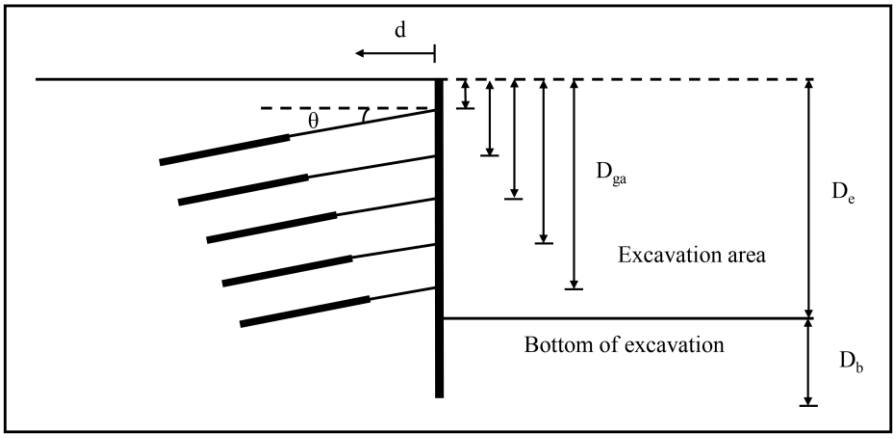

Fig. 5 The schematic section of the parameters used in the 3D FE analyses of the current study

Table 3 Values of design parameters considered in the 3D FE analyses of this research

Parameter	Unit	Values
θ	°	10, 20 and 30
D_e	m	8, 12 and 16
D_b/D_e	-	0.4, 0.6, 0.8, 1, 1.2, 1.4 and 1.8

Table 4 Different configurations of ground anchors used in the parametric studies

D_e (m)	Designation	D_{ga} (m)				
		First anchor	Second anchor	Third anchor	Fourth anchor	Fifth anchor
8	1-A	2	4	6	-	-
	1-B	2	4	7	-	-
	1-C	2	5	7	-	-
	1-D	2	5	8	-	-
12	2-A	2	4	6	9	-
	2-B	2	4	7	9	-
	2-C	2	4	7	10	-
	2-D	2	5	7	10	-
	2-E	2	5	8	10	-
	2-F	2	5	8	11	-
16	3-A	2	4	6	9	12
	3-B	2	4	7	9	12
	3-C	2	4	7	10	13
	3-D	2	5	7	10	13
	3-E	2	5	8	10	13
	3-F	2	5	8	11	14

parametric studies are shown in Table 4. In this table, D_b is Wall embedment depth and D_e represents depth of excavation as schematically demonstrated in Fig. 5. As it exhibited in Table 4, for example when D_e= 16 m (the designations 3-A to 3-F), five rows of ground anchors were considered at different positions and 3D analyses were carried corresponding to different values of D_b/D_e ratio (0.4 to 1.8, see the values illustrated in Table 3).

In all the 3D analysis performed herewith, the width of the excavation was assumed to be 30.5 m. Additionally, the depth of the model and the extent of lateral boundaries of the model from the wall were considered to be $4D_e$ and $6.7D_e$, respectively, as suggested by Shi *et al.* (2015). For example, when D_e= 16 m these values were kept 64 m and 107.2 m, respectively. The soil parameters were the same as presented in Table 1. The calculation steps in PLAXIS 3D were maintained identical to the sequences provided in Table 2 and the soil was excavated in 0.6 m increments. At the stage of installation of the ground anchors, node-to-node anchor and an embedded beam elements are activated with pre-stress forces applied to them. At D_e= 8 m, the anchors had pre-stress forces of 630 kN for the first row and 570 kN for the second and third rows. For D_e= 12 m, the pre-stress forces were 630 kN for the first two rows and 570 kN for the third and fourth rows. Lastly, at D_e= 16 m, the pre-stress forces were 630 kN for the first two rows and 570 kN for the third, fourth, and fifth rows of anchors. These values correspond to 1.33 times the design load as documented in Abraham (2007). These steps continued until the final level of the excavation was reached.

4.1 Effect of anchors inclination

One of the essential parameters in the design of tie-back walls is the inclination of ground anchors (θ). In ordinary urban excavations, the value of θ is usually considered between 10° and 20°, mainly recommended by Sabatini and Bachus (1999). Plant (1972) and Anderson and Hanna (1977) reported that by increasing the value of θ, the displacement of the retaining structure is transformed from rotational to translational. To evaluate the effect of θ on excavation response, three 3D FE analyses were carried out. In the 3D analyses the position, length, horizontal and vertical spacing of ground anchors along with other design parameters were maintained constant, while the value of θ varied in the range of 10°, 20° and 30°. The effect of θ on the horizontal displacement profiles of the wall, the surface settlement profiles and also the corresponding maximum values are illustrated in Fig. 6. It is seen that the values of δ_h

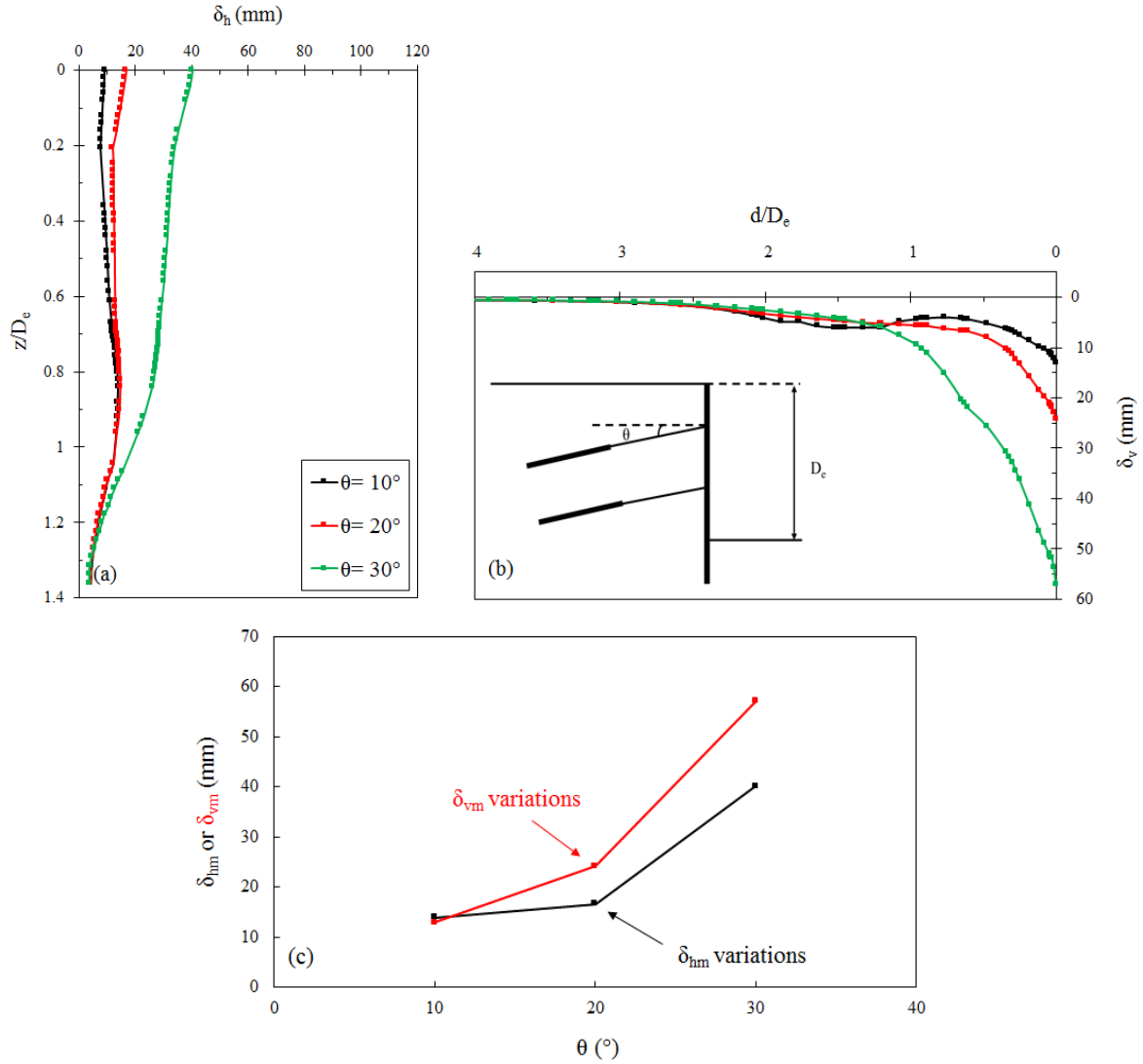

Fig. 6 Effect of anchors inclination value on; (a) the horizontal displacement profiles of the wall, (b) the surface settlement profiles and (c) δ_{hm} and δ_{vm} variations

and δ_v increase with an increase in the value of θ. Fig. 6(a), demonstrates an initial small inward displacement of 4 mm at the lowest part of the wall (z/D_e= 1.35), regardless of θ.

The differences in δ_h for θ of 10° and 20° are negligible in the lowest half of the wall while starting to deviate at almost z/D_e= 0.67 upwards, rising to 40% at the wall top. For θ= 10°, the value of δ_{hm} occurred at z/D_e= 0.84, whereas the maxima were obtained at the excavation edge for other sets. For θ= 30°, the displacements start to deviate from other sets and the maximum deformation is about 40 mm, more than four times the value corresponding to θ= 10°. Fig. 6(b) displays that the ground surface displacement is somehow insensitive to θ at distances beyond 10 m. It is further indicating that the zone of influence of settlement due to the excavation is 6.7D_e which is in sympathy with the maximum settlement. Additionally, in all three cases, the value δ_{vm} occurred at the excavation edge. The corresponding maximum values for the horizontal wall displacement and surface settlement gleaned from Figs. 6(a) and (b) are shown in Fig. 6(c). It is seen that the lowest values of δ_{hm} and δ_{vm} were reached when θ= 10°, which implies the optimum anchorage arrangements being close to a sub-horizontal condition. It also indicates that increasing the value of θ from 10° to 20° will bring about, δ_{hm} and δ_{vm} to increase by 20.71% and 79.68%, respectively while a further 10° increase in the anchor inclination will give rise to a total increase of about 141% and 136% for δ_{hm} and δ_{vm}, respectively. An implication from the observations in Fig. 6(c) is that increasing the anchors inclination will lead the horizontal and vertical components of the force mobilized in ground anchors to decrease and increase, respectively.

4.2 Effect of position of the ground anchors

To study the effects of position of the ground anchors and D_b, as schematically demonstrated in Fig. 5, a total of 112 3D FE analyses were performed. The length and inclination of ground anchors were kept constant; while the values of D_e, D_b/D_e and the anchors arrangement were varied as according to Tables 3 and 4. Furthermore,

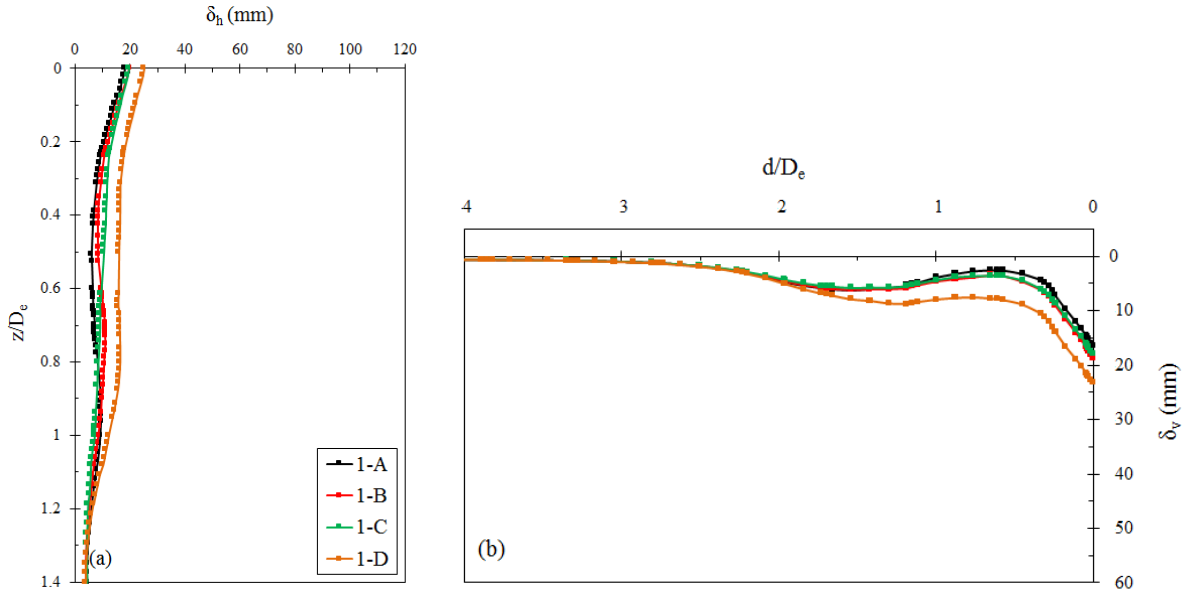

Fig. 7 Effect of anchor arrangements at D_e= 8 m and D_b/D_e= 0.4 on; (a) the horizontal displacement profile of the wall and (b) the surface settlement profile

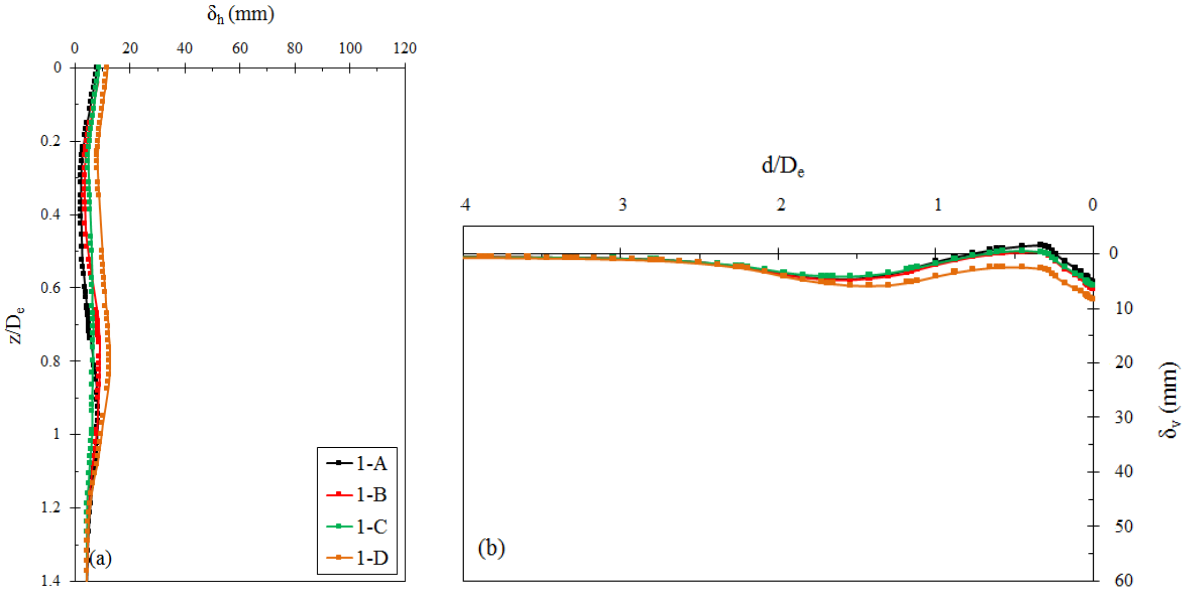

Fig. 8 Effect of anchor arrangements at D_e= 8 m and D_b/D_e= 1 on; (a) the horizontal displacement profile of the wall and (b) the surface settlement profile

according to the results obtained from section 4.1, the value of 10° for θ was chosen as a representative value since the minimum deformations were attained at this angle. Due to the large number of simulations, only the results of the horizontal displacement profiles of the wall and the surface settlement profiles in different value of D_e (8 m, 12 m and 16 m) and D_b/D_e= 0.4, 1 and 1.4 are presented in Fig. 7 to 15. Fig. 7 to 9, 10 to 12 and 13 to 15 belong to D_e= 8 m, 12 m and 16 m, respectively.

As seen in Figs. 7(a), 8(a) and 9(a), for the value of $z/D_e \geq 1.25$ m, the variation in different position systems of anchors and different values of D_b/D_e does not have a significant effect on the value of δ_h. At a certain value of D_b/D_e, the minimum value of δ_h corresponds to system 1-A, where the first, second and third row of anchors are located at 0.25, 0.50 and 0.75 of D_e below the ground level, respectively. When D_e= 8 m, the value of δ_h largely depends on the vertical distance between the last two anchors, so that the value of δ_h for systems 1-A and 1-C is less than systems 1-B and 1-D. As presented in Table 4, the vertical distance between the last two anchors in systems 1-A and 1-C are 2 m, but 3 m in systems 1-B and 1-D. As D_b/D_e

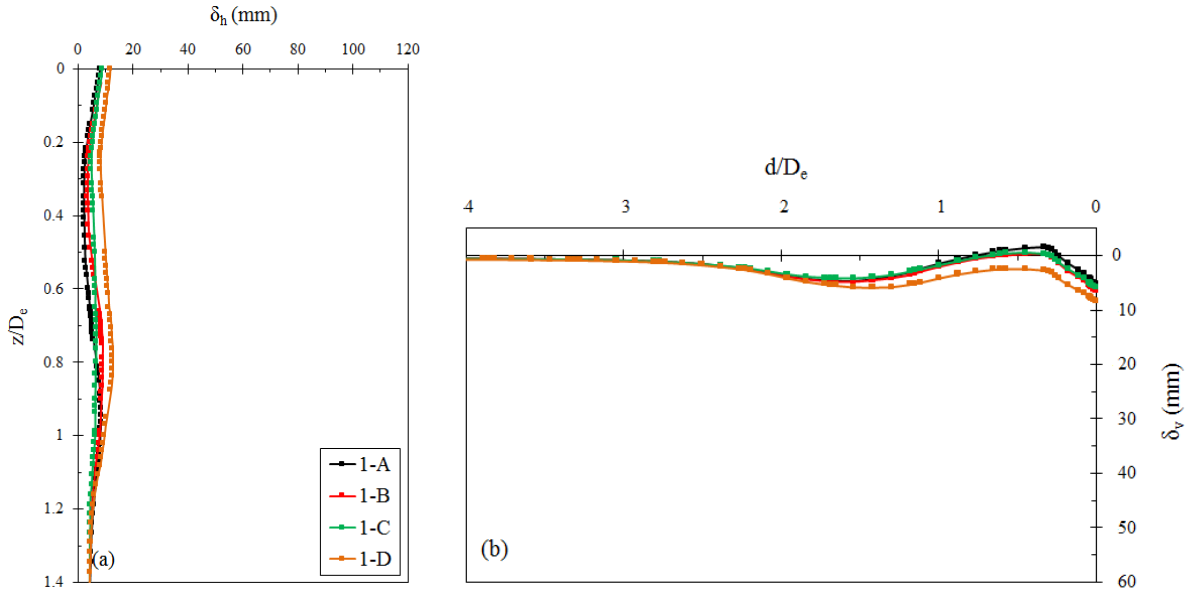

Fig. 9 Effect of anchor arrangements at D_e= 8 m and D_b/D_e= 1.4 on; (a) the horizontal displacement profile of the wall and (b) the surface settlement profile

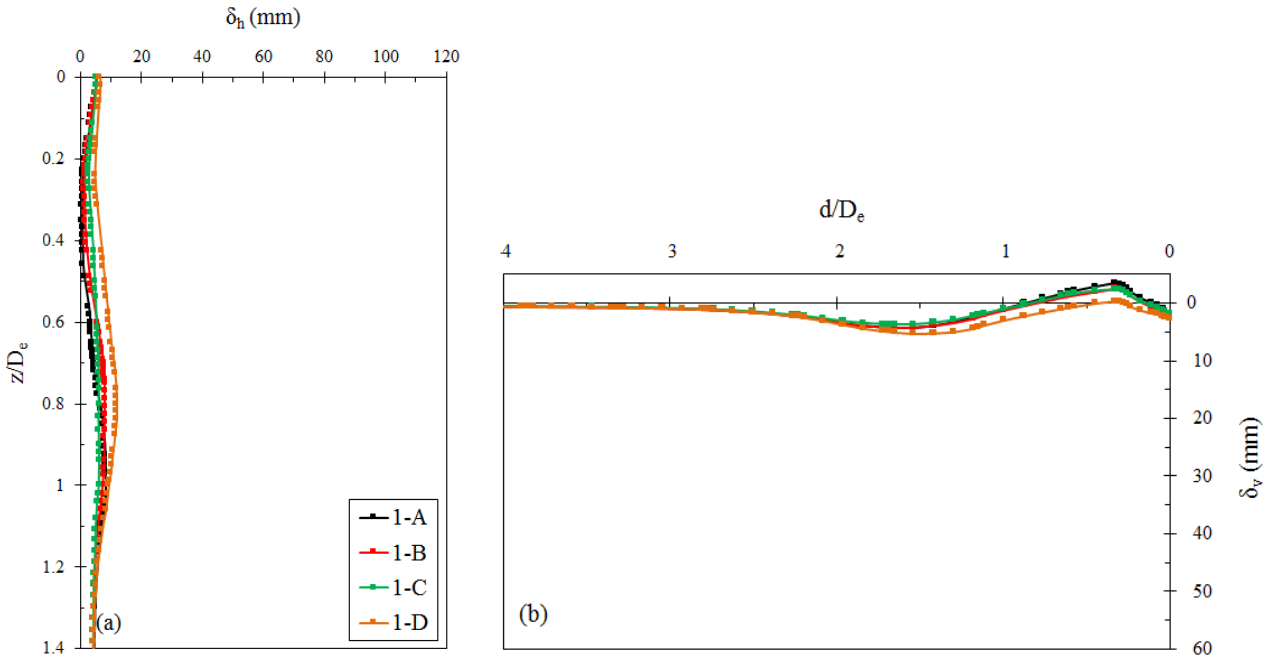

Fig. 10 Effect of anchor arrangements at D_e= 12 m and D_b/D_e= 0.4 on; (a) the horizontal displacement profile of the wall and (b) the surface settlement profile

lowers, it seems that the shape of the horizontal displacement profiles incline toward a cantilever wall and the value of δ_{hm} occurs at the tip of the wall. However, the shape of diagrams become convex by increasing the value of D_b/D_e, and the value of δ_{hm} occurs approximately in the middle 1/3 of the wall's height (see D_b/D_e= 1 in Fig. 8(a) in comparison to D_b/D_e= 0.4 in Fig. 7(a)). Additionally, it is seen that as the value of D_b/D_e increases, the value of δ_h created at the edge of the wall reduces.

As shown in Figs. 7(b), 8(b) and 9(b), for the value of $d/D_e \geq 3.125$, the variation in different positions of anchors at identical values of D_b/D_e do not have a significant effect on the values of δ_v. In three values of D_b/D_e, the value of δ_v obtained from system 1-D is greater than systems 1-A, 1-B and 1-C. By increasing the value of D_b/D_e, a modest heave occurs near the edge of the wall (0.375 m $\leq d/D_e \leq$ 1 m), which for system 1-A in D_b/D_e= 1.4, the heave value is higher than other systems. Furthermore, as the value of

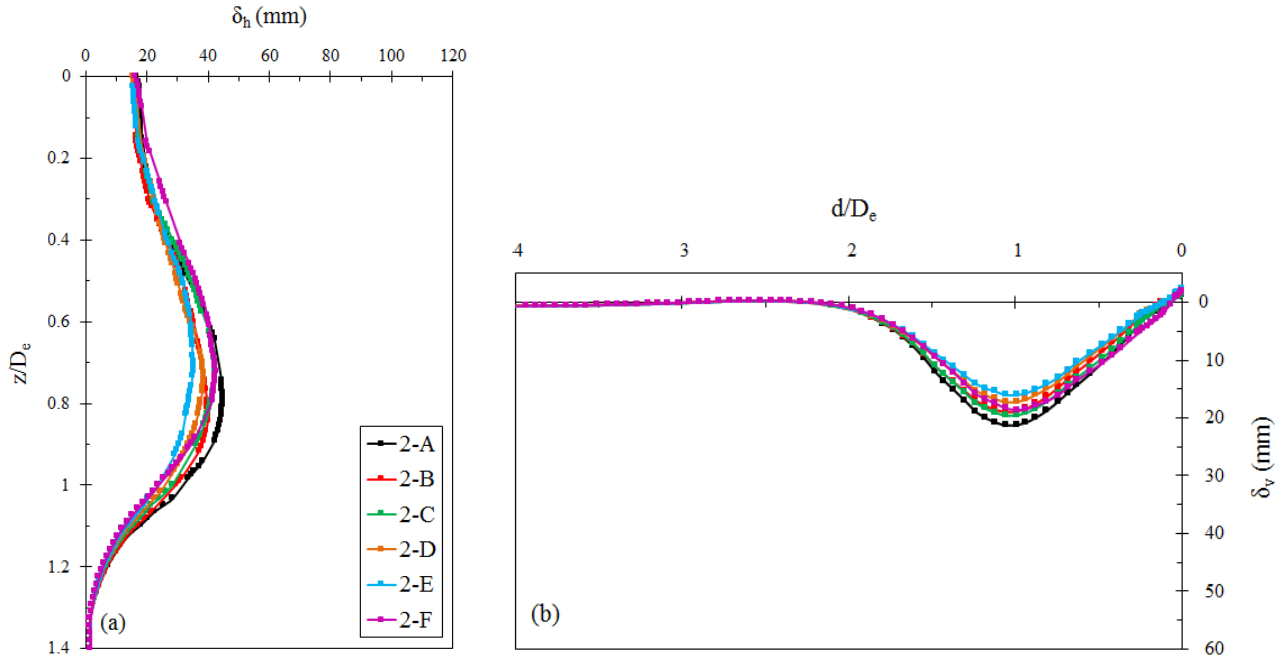

Fig. 11 Effect of anchor arrangements at D_e= 12 m and D_b/D_e= 1 on; (a) the horizontal displacement profile of the wall and (b) the surface settlement profile

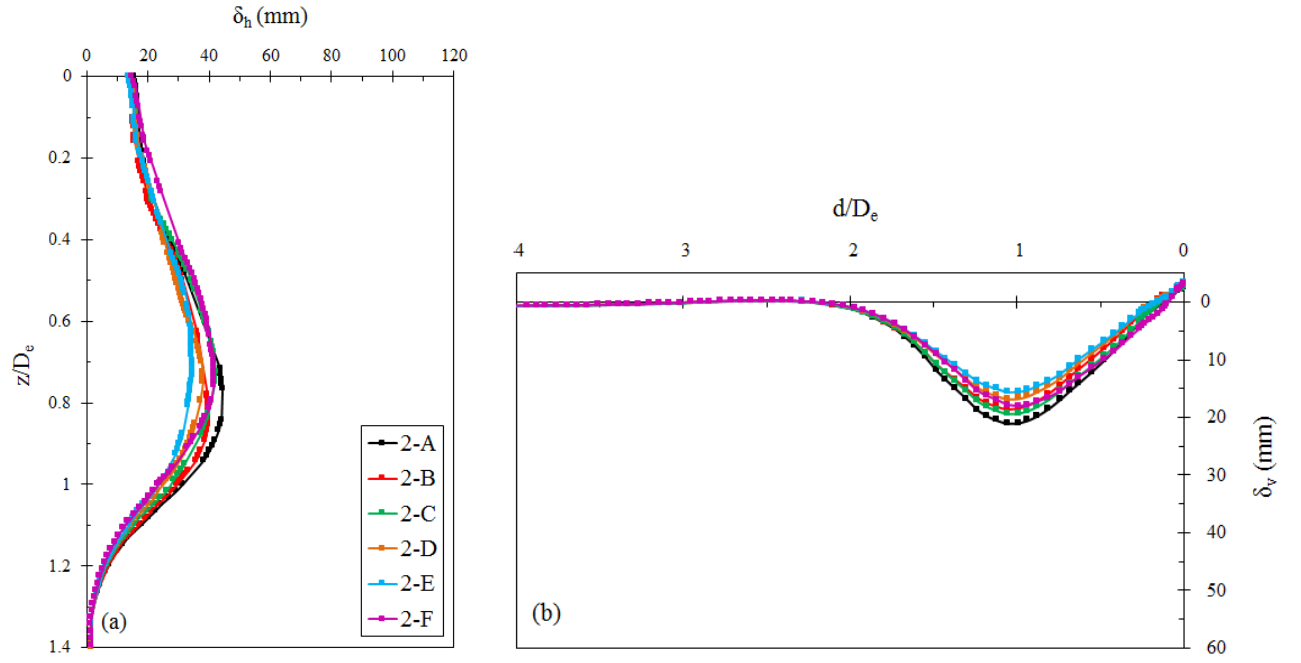

Fig. 12 Effect of anchor arrangements at D_e= 12 m and D_b/D_e= 1.4 on; (a) the horizontal displacement profile of the wall and (b) the surface settlement profile

D_b/D_e increases, the surface settlement regime changes and as the value of δ_v decreases, the amount of heave proportionally increases.

Comparison of the sets of plots illustrated in Figs. 7(a)-9(a) and Figs. 10(a)-12(a) reveals that as the value of D_e increases from 8 m to 12 m, the wall behavior changes at shallow depths. In other words, it is evident from the comparison that the maximum horizontal wall movement moves from the upper shallow depths to the lower half. This is evident as increasing the wall height brings about more flexibility in the wall behavior substantiated in the form of nonlinear wall deformation profile bulging at deeper areas.

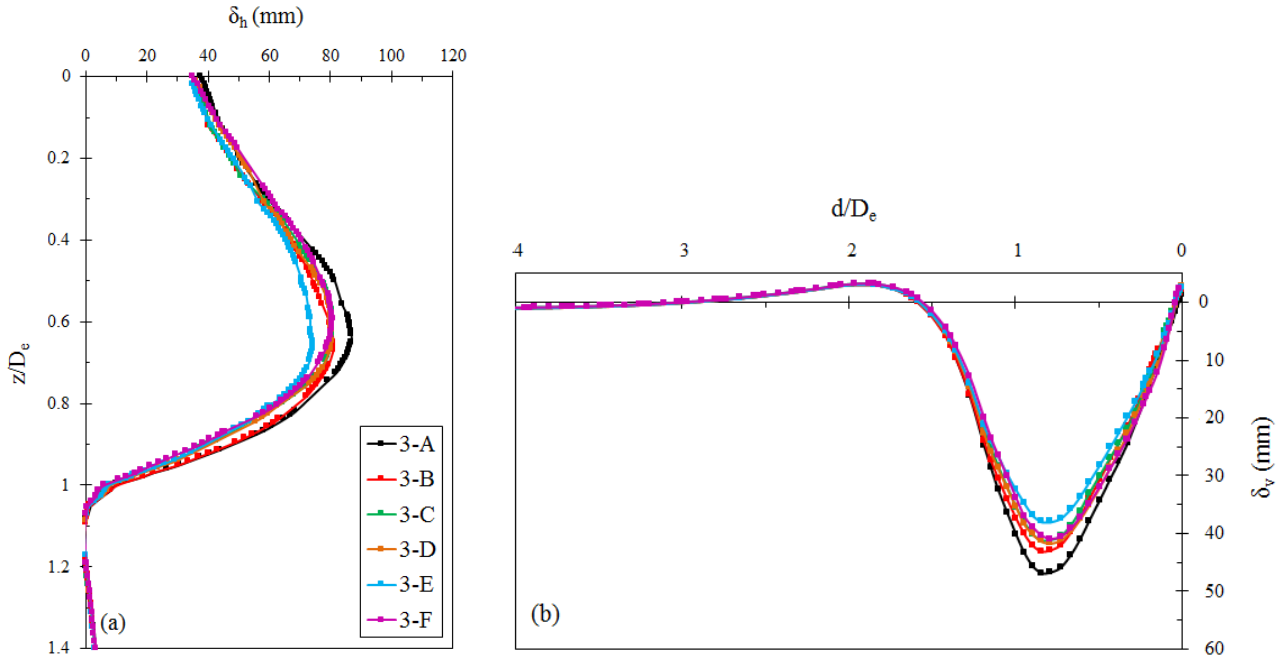

Fig. 13 Effect of anchor arrangements at D_e= 16 m and D_b/D_e= 0.4 on; (a) the horizontal displacement profile of the wall and (b) the surface settlement profile

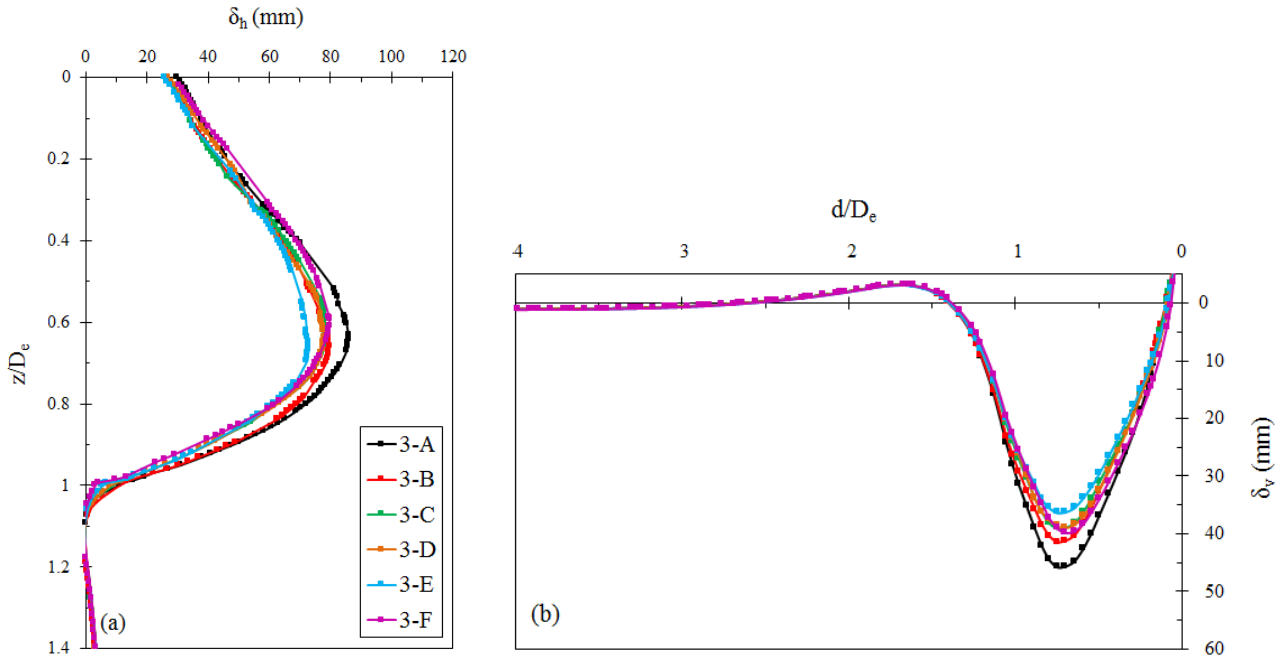

Fig. 14 Effect of anchor arrangements at D_e= 16 m and D_b/D_e= 1 on; (a) the horizontal displacement profile of the wall and (b) the surface settlement profile

It is further observed that at a certain embedment depth ratio D_b/D_e, the minimum value of δ_h corresponds to the system 2-E, where the first, second, third and fourth row of anchors are located at 0.17, 0.41, 0.67 and 0.83 D_e below the ground level, respectively. This bear witness to the very fact that the anchors configuration in system 2-E provides more anchorage around the zone of maximum horizontal deformation which is z/D_e = 0.83.

Figs. 10(b)-12(b) demonstrate that for the distance beyond d/D_e = 2.083 from the excavation facing, the variety in configuration of anchors and embedment ratio of D_b/D_e does not have a significant effect on the value of δ_v. They

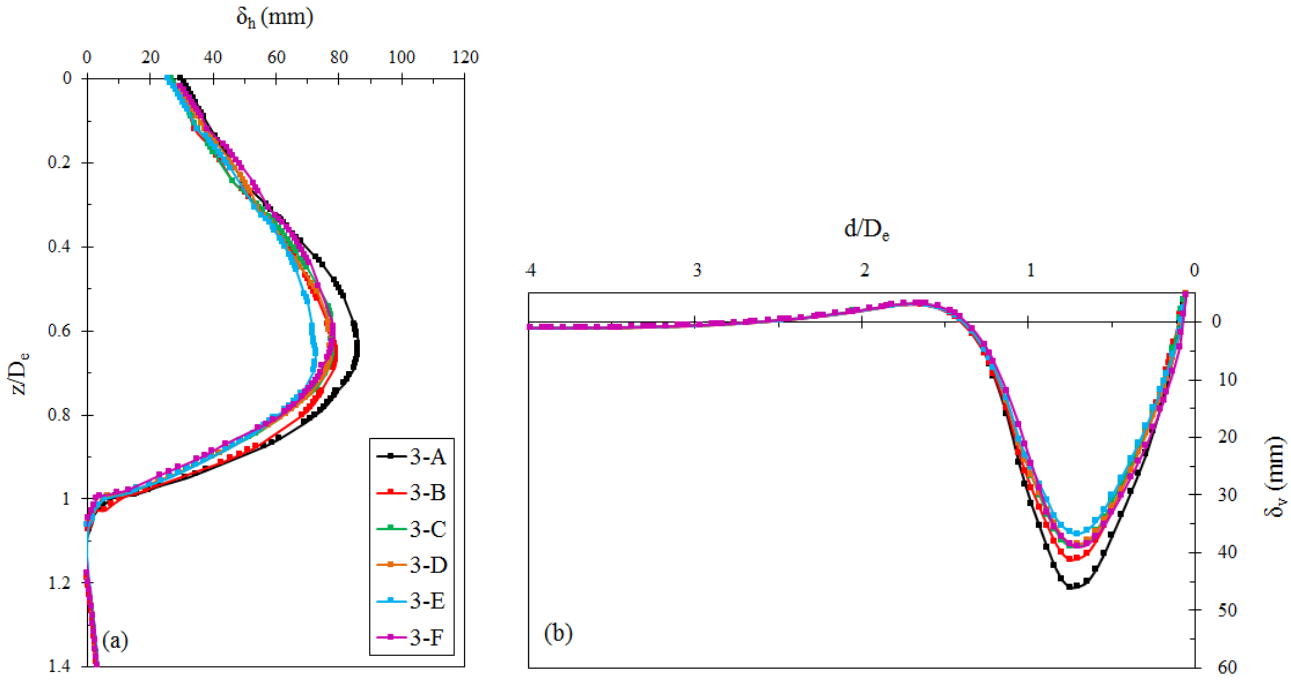

Fig. 15 Effect of anchor arrangements at D_e= 16 m and D_b/D_e= 1.4 on; (a) the horizontal displacement profile of the wall and (b) the surface settlement profile

also show that the value of δ_v obtained from the system 2-E is less than the others. As seen, the ground surface settlement curves are concave and δ_{vm} occurs at around 12 m, which is equivalent to d/D_e = 1. For the value of D_b/D_e of 1 and beyond an insignificant heave occurs near the edge of the wall with magnitudes being less than 5 mm. Another observation from Figs. 10(a)-12(a) is that providing embedment depth D_b/D_e beyond 1 offers no more benefit in terms of improving performance of the system.

From Figs. 13(a)-15(a), all belonging to the excavation depth of 16 m, it is evident that the horizontal displacement profile of the wall is convex shape, like the corresponding plots for the cases of D_e= 12 m. For all D_b/D_e ratios, the minimum and maximum values of δ_h correspond to the systems 3-E and 3-A, respectively.

Figs. 13(b)-15(b), on the other hand, showed that for D_e= 16 m, the type of the surface settlement profile remains concave upward like type in the case of D_e= 12 m. Again the results corroborate that at a certain of D_b/D_e ratio, the minimum and maximum δ_v values correspond to the systems 3-E and 3-A, respectively.

4.3 Effect of Wall embedment depth (D_b)

Fig. 16, illustrates the effect of the non-dimensional parameter D_b/D_e on the maximum horizontal and vertical deformations. It indicates that the values of δ_{hm} and δ_{vm} increase by an increase in the value of D_e. Additionally, changes in the D_b/D_e are more obviously reflected on δ_{hm} and δ_{vm} for the case of D_e= 8 m (compare the variations of black diagrams vs. green and red colors diagrams). The values of δ_{hm} and δ_{vm} diminish by increasing the D_b/D_e ratio to a threshold value and to level off afterwards. It should be noted that for all values of D_e and D_b/D_e ratio considered in this study (8 m, 12 m, and 16 m), the values of maximum lateral wall movements and maximum vertical settlements behind the wall are lower than the values recommended in FHWA-SA-99-015 (δ_{hm} and δ_{vm} < 0.50% H, where H represents the wall height).

When D_e= 8 m, the values of δ_{hm} and δ_{vm} of the system 1-Dother counterparts (1-A, 1-B and 1-C). The value of δ_{vm} for t is greater than the he system 1-D corresponding to D_b/D_e= 0.4 and 0.6 coincides with these in the system 2-E at D_e= 12 m. Fig. 16 shows that for the values of $D_b/D_e \geq$ 1.2, the embedment depth has actually no significant influence on the wall deformations. Therefore, at D_e= 8 m, the ratio of 1.2 seems to be as the optimum value for D_b/D_e. When D_e= 12 m, the minimum and maximum values of δ_{hm} and δ_{vm} corresponds to the systems 2-E and 2-A, respectively. In the system 2-A, the first, second, third and fourth row of anchors are located at 0.17, 0.33, 0.50 and 0.75 D_e below the ground level, respectively. The results clearly show that, as the value of D_e increases from 8 to 12 m, the optimum ratio of D_b/D_e decreases significantly. As seen in Fig. 16, for the values of $D_b/D_e \geq$ 0.60 in the systems 2-A to 2-F, D_b/D_e has no effect on the values of δ_{hm} and δ_{vm}. When D_e= 16 m, the results show that the systems 3-E and 3-A have the best and the worst performance in terms of wall deformations, respectively. In the system 3-E, the first, second, third, fourth and fifth row of anchors are located at 0.12, 0.31, 0.50, 0.62 and 0.81 D_e below the ground level but in the system 3-A, the first, second, third, fourth and fifth row of anchors are located at 0.12, 0.25, 0.33, 0.56 and 0.67 D_e below the ground level, respectively. In addition,

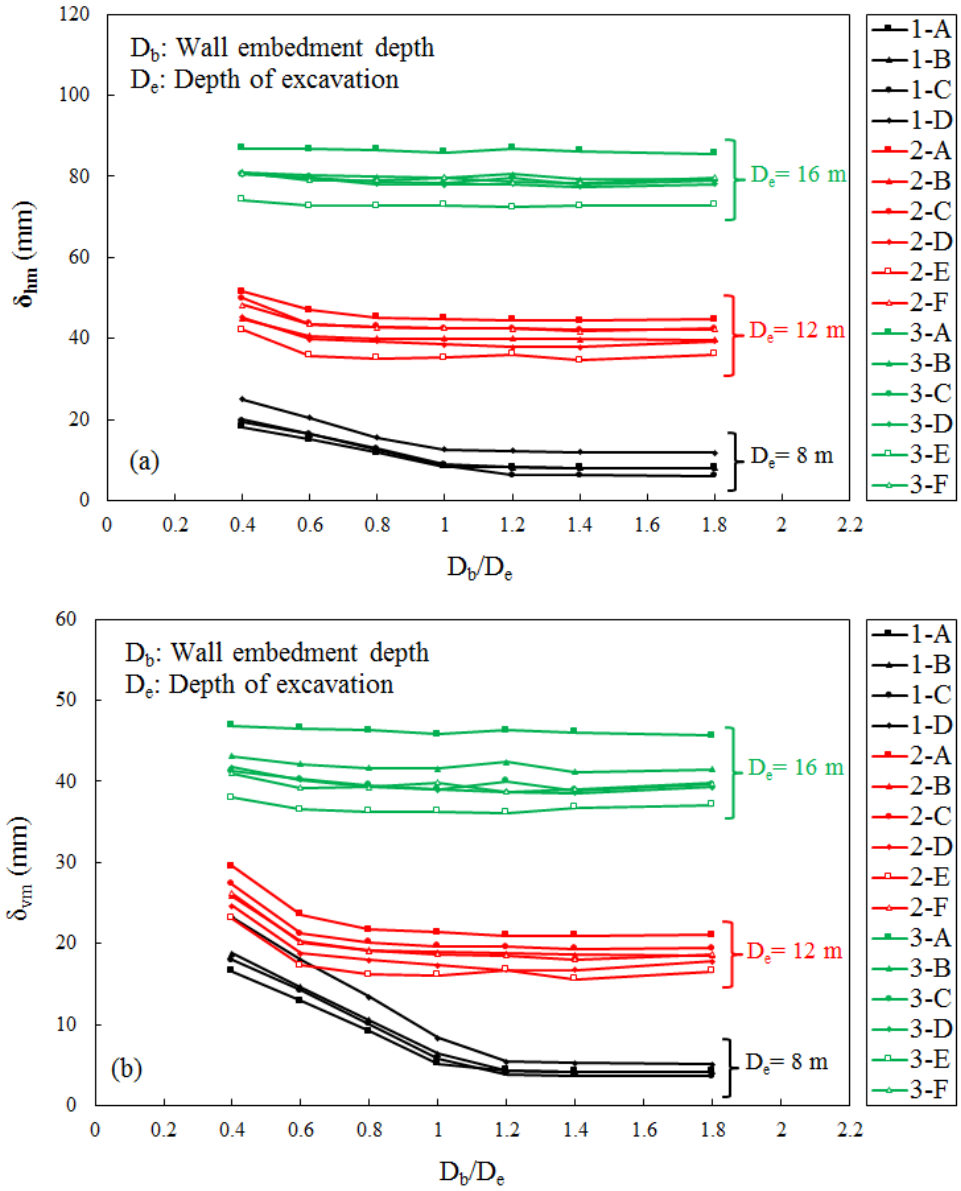

Fig. 16 Effect of D_b/D_e on; (a) maximum horizontal displacement of the wall, δ_{hm}; and (b) Maximum surface settlement, δ_{vm}

changes in the configuration of the ground anchors in the systems 3-C, 3-D and 3-F have no effect on the values of δ_{hm} and δ_{vm} and they are almost identical for these systems. Similar to the case of D_e= 12 m, for D_e= 16 m, the value of D_b/D_e= 0.60 seems to be the optimum value. The results in Fig. 16 also show that a change in the value of D_b/D_e alters the values of δ_{vm} more abruptly than δ_{hm}.

5. Simplified model for estimation excavation deformations

As presented earlier, for D_e= 8, 12 and 16 m, by increasing the ratio of D_b/D_e to a certain ratio, the values of δ_{hm} and δ_{vm} reduce and then remain unwavering. Based on the 3D numerical modeling results obtained here and least-squares method, two following simple equations are developed to estimate the average maximum horizontal displacement of the wall ($\delta_{hm\ (av)}$) and average maximum surface settlement ($\delta_{vm\ (av)}$), respectively

$$\delta_{hm\ (av)} = 8.381\ (D_e) - 4.384\ (\frac{D_b}{D_e}) - 51.6 \qquad (1)$$

$$\delta_{vm\ (av)} = 3.93\ (D_e) - 5.304\ (\frac{D_b}{D_e}) - 18.4 \qquad (2)$$

It should be noted that the range of parameters used in Eqs. (1) and (2) are the same as those illustrated in Tables 3 and 4.

To verify the robustness developed model, the results obtained from Eqs. (1) and (2) are compared with those from FE results. Fig. 17 displays the performance of the

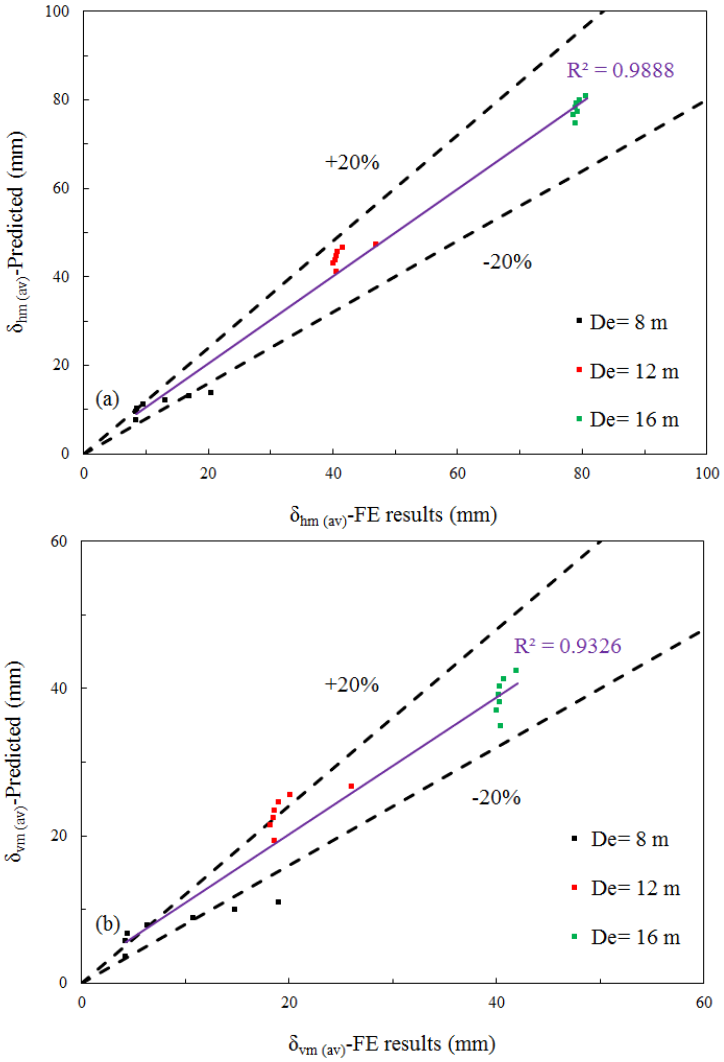

Fig. 17 Performance of Eqs. (1) and (2) versus FE results; (a) $\delta_{hm\ (av)}$ and (b) $\delta_{vm\ (av)}$

proposed equations in reproducing the values of $\delta_{hm\ (av)}$ and $\delta_{vm\ (av)}$. The horizontal and vertical axes of the charts presented in Fig. 17 are the values of $\delta_{hm\ (av)}$ and $\delta_{vm\ (av)}$ obtained from the FE results and the predicted values, respectively. As seen in these diagrams, reliability of the proposed equations to determine the values of $\delta_{hm\ (av)}$ and $\delta_{vm\ (av)}$ is reflected in value of R^2, which is close to one, all indicating the high accuracy of the developed model.

The relationship between the calculated values of δ_{hm} and δ_{vm} are illustrated in Fig. 18. From Fig. 15 it is clearly observed that the FE values of δ_{vm} are smaller than δ_{hm}. Ou (2006) proposed δ_{vm}= 0.5 δ_{hm} for sandy soils and the δ_{vm}= δ_{hm} for clays, and somewhere between the two for soils in between. The results of FE analysis of this study showed that δ_{vm}= (0.4-1) δ_{hm}.

6. Conclusions

This research presents the results of 116 3D FE models of a deep excavation supported by tie-back wall system. The obtained results were compared against those from measurement and the results presented by Briaud and Lim (1999) to validate the accuracy of the numerical results.

Then, the significant parameters of design, deemed to affect the excavation deformations the most, were investigated. Eventually, based on the 3D numerical results, two simple mathematical equations were presented to enable estimating the values of δ_{hm} and δ_{vm}. The concluding remarks are as follows:

- 3D FE is found to robust enough to predict the behavior of a deep excavation to an acceptable degree.
- The values of δ_{hm} and δ_{vm} increase by increasing the value of θ. Moreover, δ_{hm} was found to be more sensitive θ as compared to δ_{vm}.
- For the value of 0 m<D_e≤8 m, the value of δ_h largely depends on the vertical distance between the last two anchors. The minimum value of δ_h are related to the case where these two are installed around z=10 m.
- For the value of 8 m<D_e≤12 m, if the first, second, third and fourth rows of ground anchors are located at 0.17, 0.41, 0.67 and 0.83 D_e below the ground level, respectively, an optimum results are obtained.
- For the value of 12 m<D_e≤16 m, the first, second, third, fourth and fifth row of anchors are located at 0.12,

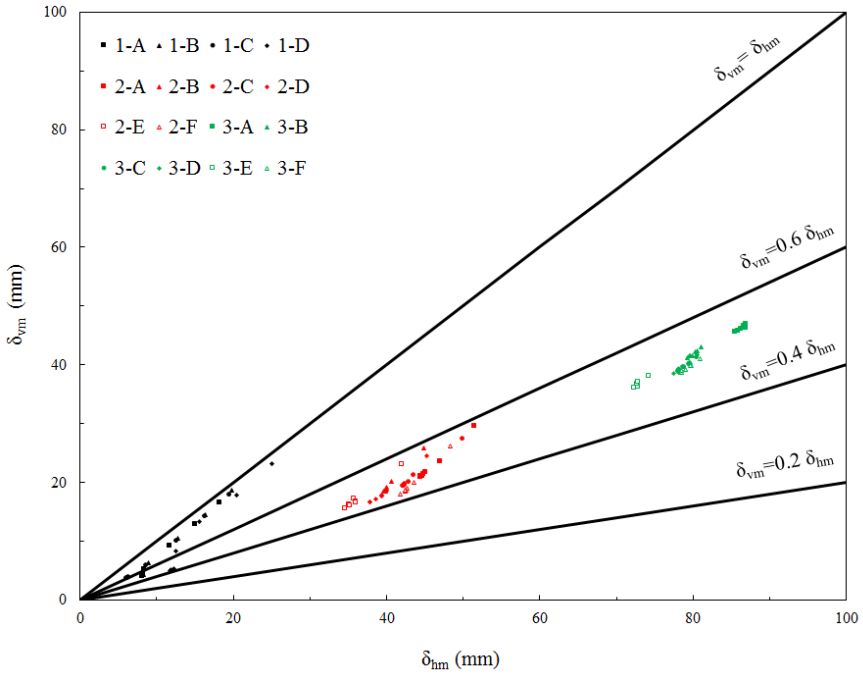

Fig. 18 8 The relationship between the calculated values of δ_{hm} and δ_{vm} in the current study

0.31, 0.50, 0.62 and 0.81 D_e below the ground level, respectively, an optimum result is expected.

- The values of δ_{hm} and δ_{vm} reduce by an increase in the value of D_b/D_e to a certain value and then to remain approximately the same. Results of the numerical analyses showed that embedment ratios D_b/D_e= 1.2, and 0.6 can be assumed as the optimum embedment ration for D_e= 12 m and 16 m, respectively.
- It was shown that the D_b/D_e ratio has more notable influence on δ_{vm} than on δ_{hm}.
- Comparison between the results obtained from FE analyses and the simple equations proved a high accuracy of the proposed equations. Therefore, the developed regression-based model can be adopted for serviceability limit design of tie-back wall system in deep urban excavations for projects involving similar construction and soil conditions.

References

Abraham, K. (2007), "Three dimensional behavior of retaining wall system." PhD thesis, Department of Civil Engineering, Louisiana State.

Ahmadi, A. and Ahmadi, M.M. (2019), "Three-dimensional numerical analysis of corner effect of an excavation supported by ground anchors", *Int. J. Geotech. Eng.*, **16**(7), 903-915. https://doi.org/10.1080/19386362.2019.1682349.

Anderson, W.F. and Hanna, T.H. (1977), "Model tests on anchored walls retaining overconsolidated sands", Department of Civil Engineering, the University Mappin, Sheffield, England.

Blackburn, J.T. (2005), "Automated sensing and three-dimensional analysis of internally braced excavations", PhD Thesis, Northwestern University, Evanston, IL.

Bono, N.A., Liu, T.K. and Soydemir, C. (1992), "Performance of an internally braced slurry-diaphragm wall for excavation support", Slurry walls: Design, construction, and quality control, ASTM STP 1129. (Eds., D.B. Paul, R.G. Davidson, and N. J. Cavalli), ASTM, Philadelphia, 169-190.

Borges, J.L. and Guerra, G.T. (2014), "Cylindrical excavations in clayey soils retained by jet grout walls: Numerical analysis and parametric study considering the influence of consolidation", *Comput. Geotech.*, **55**, 42-56. https://doi.org/10.1016/j.compgeo.2013.07.008.

Briaud, J.L. and Lim, Y. (1999), "Tieback walls in sands: numerical simulation and design implications", *J. Geotech. Geoenviron. Eng.*, **125**(2), 101-110. https://doi.org/10.1061/(ASCE)1090-0241(1999)125:2(101).

Chew, S.H., Yong, K.Y. and Lim, A.Y.K. (1997), "Three-dimensional finite-element analysis of a strutted excavation." Computer methods and advanced in geomechanics, Yuan, Ed., Balkema, Rotterdam, The Netherlands.

Chheng, C.H. and Likitlersuang, S. (2018), "Underground excavation behaviour in Bangkok using three-dimensional finite element method", *Comput. Geotech.*, **95**, 68-81. https://doi.org/10.1016/j.compgeo.2017.09.016.

Chowdhury, S.S., Deb, K. and Sengupta, A. (2012), "Estimation of design parameters for braced excavation: numerical study", *Int. J. Geomech.*, **13**(3), 234-247. https://doi.org/10.1061/(ASCE)GM.1943-5622.0000207.

Chowdhury, S.S., Deb, K. and Sengupta, A. (2016), "Effect of fines on behavior of braced excavation in sand: experimental and numerical study", *Int. J. Geomech.*, **16**(1), 04015018-13. https://doi.org/10.1061/(ASCE)GM.1943-5622.0000487.

Chung, M. and Briaud, J.L. (1993), "Behavior of a full scale tieback wall in sand", Rep. to Schnabel Foundation and the Federal Highway Administration, Department of Civil Engineering Texas A&M University, College Station, Texas.

Clough, G.W. and Tsui, Y. (1974), "Performance of tied-back walls in clay", *J. Geotech. Eng. Division ASCE*, Vol. 100, Nom GT12, 1259-1273. https://doi.org/10.1061/AJGEB6.0000128.

Comodromos, E.M., Papadopoulou, M.C. and Konstantinidis,

G.K. (2013), "Effects from diaphragm wall installation to surrounding soil and adjacent buildings", *Comput. Geotech.*, **53**, 106-121. https://doi.org/10.1016/j.compgeo.2013.05.003.

Dawkins, W.P., Storm, R.W. and Ebeling, R.M. (2003), "User's Guide: Computer program for simulation of construction sequence for stiff wall systems with multiple levels of anchors (CMULTIANC)", Instruction Report ITL-U.S. Army Engineer Research and Development Center, Vickburg, MS.

Ding, Z.H., Wei, X.J. and Wei, G. (2017), "Prediction methods on tunnel-excavation induced surface settlement around adjacent building", *Geomech. Eng.*, **12**(2), 185-195. https://doi.org/10.12989/gae.2017.12.2.185.

Finno, R.J. and Bryson, L.S. (2002), "Response of a building adjacent to stiff excavation support system in soft clay", *J. Perform. Constr. Fac.*, **16**(1), 10-20. https://doi.org/10.1061/(ASCE)0887-3828(2002)16:1(10).

Finno, R.J. and Roboski, J.F. (2005), "Three-dimensional responses of a tied-back excavation through clay", *J. Geotech. Geoenviron. Eng. - ASCE*, **131**(3), 273-282. https://doi.org/10.1061/(ASCE)1090-0241(2005)131:3(273).

Hou, Y.M., Wang, J.H. and Zhang, L.L. (2009), "Finite-element modeling of a complex deep excavation in shanghai", *Acta Geotechnica*, 4(1), 7-16. https://doi.org/10.1007/s11440-008-0062-3.

Huang, X., Schweiger, H.F. and Huang, H. (2013), "Influence of deep excavations on nearby existing tunnels", *Int. J. Geomech.*, **13**(2), 170-180. https://doi.org/10.1061/(ASCE)GM.1943-5622.0000188.

Ignat, R., Baker, S., Larsson, S. and Liedberg, S. (2015), "Two- and three-dimensional analyses of excavation support with rows of dry deep mixing columns", *Comput. Geotech.*, **66**, 16-30. https://doi.org/10.1016/j.compgeo.2015.01.011.

Karira, H., Kumar, A., Hussain Ali, T., Ali Mangnejo, D. and Mangi, N. (2022), "A parametric study of settlement and load transfer mechanism of piled raft due to adjacent excavation using 3D finite element analysis", *Geomech. Eng.*, **30**(2), 169-185. https://doi.org/10.12989/gae.2022.30.2.169.

Kim, J., Kim, J., Lee, J. and Yoo, H. (2018), "Prediction of transverse settlement trough considering the combined effects of excavation and groundwater depression", *Geomech. Eng.*, **15**(3), 851-859. https://doi.org/10.12989/gae.2018.15.3.851.

Kung, G.T.C. (2009), "Comparison of excavation-induced wall deflection using top-down and bottom-up construction methods in Taipei silty clay", *Comput. Geotech.*, **36**, 373-385. https://doi.org/10.1016/j.compgeo.2008.07.001.

Lee, S.K. (2019), "Experimental study on effect of underground excavation distance on the behavior of retaining wall", *Geomech. Eng.*, **17**(5), 413-420. https://doi.org/10.12989/gae.2019.17.5.413.

Liu, B., Yu, Zh., Xue, Y., Han, Y., Wang, Zh., Yang, SH. and Liu, H. (2020), "A simplified combined analytical method for evaluating the effect of deep surface excavations on the shield metro tunnels", *Geomech. Eng.*, **23**(5), 405-418. https://doi.org/10.12989/gae.2020.23.5.405.

Mosher, R.L. and Knowles, V.R. (1990), "Finite analysis study of tieback wall for Bonneville navigation lock", Technical Report ITL-90-4, U.S. Army Engineer Waterways Experiment Station, Vicksburg, Ms.

Muntohar, A.S. and Lio, H.J. (2013), "Finite element analysis of the movement of the tie-back wall in alluvial-silty soils", *Procedia Eng.*, **54**, 176-187. https://doi.org/10.1016/j.proeng.2013.03.017.

Ning, Z., Su, M., Xue, Y., Qiu, D., Li, Z.H. and Fu, K. (2021), "Reevaluation of the design and excavation of underground oil storage cavern groups using numerical and monitoring approaches", *Geomech. Eng.*, **27**(3), 291-307. https://doi.org/10.12989/gae.2021.27.3.291.

Orazalin, Z.Y. (2012), "Three-dimensional finite element analysis of a complex excavation on the MIT compus", MSC thesis, Department of Civil and Environmental Engineering, Massachusetts institute of technology, Cambridge, MA.

Ou, C.Y., Chiou, D.C. and Wu, T.S. (1996), "Three-dimensional finite element analysis of deep excavations", *J. Geotech. Geoenviron. Eng.*, **122**(5), 337-345. https://doi.org/10.1061/(ASCE)0733-9410(1996)122:5(337).

Ou, C.Y. and Shiau, B.Y. (1998), "Analysis of the corner effect on excavation behaviors", *Can. Geotech. J.*, **35**(3), 532-540. https://doi.org/10.1139/T98-013.

Ou, C.Y., Shiau, B.Y. and Wang, I.W. (2000), "Three-dimensional deformation behavior of the Taipei National Enterprise Center (TNEC) excavation case history", *Can. Geotech. J.*, **37**(2), 438-448. https://doi.org/10.1139/cgj-37-2-438.

Ou, C.Y. (2006), "Deep excavation theory and practice", Taylor & Francis/Balkema, London.

Plant, G.W. (1972), "An assessment of multi – anchored retaining wall behavior", PhD Thesis, University of Sheffield, England.

PLAXIS (2020), "Reference manual, Connect edition V20.04." Bentley.

Roboski, J.F. and Finno, R.J. (2006), "Distributions of ground movements parallel to deep excavations in clay", *Can. Geotech. J.*, **43**(1), 43-58. https://doi.org/10.1139/t05-091.

Sabatini, P.J. and Bachus. D.G. and Bachus, R.C. (1999), "Ground anchors and anchored systems", *Geotechnical Engineering Circular No. 4*, FHWA-SA-99-015.

Sarfarazi, V. and Tabaroei, A. (2020), "Numerical simulation of the influence of interaction between Qanat and tunnel on the ground settlement", *Geomech. Eng.*, **23**(5), 455-466. https://doi.org/10.12989/gae.2020.23.5.455.

Sarfarazi, V., Tabaroei, A. And Asgari, K. (2022), "Discrete element modeling of strip footing on geogrid-reinforced soil", *Geomech. Eng.*, **29**(4), 435-449. https://doi.org/10.12989/gae.2022.29.4.435.

Shi, J.W., Liu, G.B., Huang, P. and Ng, C.W.W. (2015), "Interaction between a large-scale triangular excavation and adjacent structures in Shanghai soft clay", *Tunn. Undergr. Sp. Tech.*, **50**, 282-295. https://doi.org/10.1016/j.tust.2015.07.013.

Simpson, B., O'Rioran, N.J., and Croft, D.D. (1979), "A computer model for the analysis of ground movement in London clay", *Geotechnique*, **29**(2), 149-175.

Tabaroei,. A. and Ghazavi, M. (2013), "Optimize the placement of nails in soil nailing by three dimensional numerical modeling", *Proceedings of the 7th International Symposium on Advances in Science and Technology*.

Tabaroei, A., Sarfarazi, V., Pouraminian. M. and Mohammadzadeh, S.D. (2022), "Evaluation of behavior of a deep excavation by three-dimensional numerical modeling", *Periodica Polytechnica Civil Eng.*, **66**(3), 967-977. https://doi.org/10.3311/PPci.20353.

Tabaroei, A., Seyedi, S.T. and Pouraminian, M. (2023), "Performance of a deep excavation reinforced by soil-nailing during an earthquake excitation", *Iran J. Sci. Technol. Trans. Civ. Eng.*, **47**, 3021-3031. https://doi.org/10.1007/s40996-023-01094-x.

Wang, J., Li, W., Rui, R., Zhai, Y. and He, Q. (2023), "Experimental investigation of earth pressure on retaining wall and ground settlement subjected to tunneling in confined space", *Geomech. Eng.*, **32**(2), 179-191. https://doi.org/10.12989/gae.2023.32.2.179.

Weatherby, D.E., Chung, M., Kim, N.K. and Briaud, J.L. (1998), "Summary report of research on permanent ground anchor walls, Volume II: Full-scale wall tests and a soil-structure interaction model", McLean, VA, Federal highway administration.

Yoo, C.H. and Lee, D. (2008), "Deep excavation-induced ground

surface movement characteristics – A numerical investigation", *Comput. Geotech.*, **35**, 231-252. https://doi.org/10.1016/j.compgeo.2007.05.002.
Zdrakovic, L., Potts, D.M. and John, H.D.S. (2005), "Modeling of a 3D excavation in finite element analysis", *Geotechnique*, **55**(7), 497-513.

CC

Notation

The following symbols are used in the paper:
γ= Unit weight of soil;
c= Cohesion;
φ= Internal friction angle;
E_{50}^{ref} = Reference secant stiffness from triaxial compression tests;
E_{oed}^{ref} = Reference secant stiffness from one-dimensional compression tests;
E_{ur}^{ref} = Reference secant stiffness for unloading/reloading stiffness;
m= Power component for the stress level dependency of stiffness;
ν= Poisson's ratio for unloading/reloading;
R_f= Failure ratio;
R_{int}= Interface reduction factor;
d= Distance from the wall;
D_b= Wall embedment depth;
D_e= Depth of excavation;
D_{ga}= Depth of each ground anchor below the ground level;
z= Depth;
δ_h= Horizontal displacement of the wall;
δ_{hm}= Maximum horizontal displacement of the wall;
$\delta_{hm\ (av)}$= Average of maximum horizontal displacement of the wall;
δ_v= Surface settlement;
δ_{vm}= Maximum surface settlement;
$\delta_{vm\ (av)}$= Average of maximum surface settlement;
θ= Angle of ground anchors relative to the horizon;
R^2= Coefficient of determination